

Negative spin Hall angle and large spin-charge conversion in thermally-evaporated chromium thin films

S. M. Bleser,¹ R. M. Greening,¹ M. J. Roos,¹ L. A. Hernandez,¹ X. Fan,¹ and B.L. Zink^{1, a)}

Department of Physics and Astronomy, University of Denver, Denver, Colorado 80208.

(Dated: 25 February 2022)

Spin-to-charge conversion, and the reverse process, are now critically important physical processes for a wide range of fundamental and applied studies in spintronics. Here we experimentally demonstrate effective spin-to-charge conversion in thermally evaporated chromium thin films using the longitudinal spin Seebeck effect (LSSE). We present LSSE results measured near room temperature for Cr films with thicknesses from 2 nm to 11 nm, deposited at room temperature on bulk polycrystalline yttrium-iron-garnet (YIG) substrates. Comparison of the measured LSSE voltage, V_{LSSE} , in Cr to a sputtered Pt film at the same nominal thickness grown on a matched YIG substrate shows that both films show comparably large spin-to-charge conversion. As previously shown for other forms of Cr, the LSSE signal for evaporated Cr/YIG shows the opposite sign compared to Pt, indicating that Cr has a negative spin Hall angle, θ_{sh} . We also present measured charge resistivity, ρ , of the same evaporated Cr films on YIG. These values are large compared to Pt, and comparable to β -W at similar thickness. Non-monotonic behavior of both ρ and V_{LSSE} with film thickness suggests that spin-to-charge conversion in evaporated Cr, which we expect has a different strain state than previously investigated sputtered films, could be modified by the spin density wave antiferromagnetism in Cr.

^{a)}Electronic mail: barry.zink@du.edu.

I. INTRODUCTION

The ability to generate a detectable charge voltage in response to presence of a spin current, a flow of angular momentum in a material that can be mediated by either electrons or magnons, is one of the most important tools of current spintronics research. The inverse process, which should result from the same physical processes due to time-reversal symmetry, is equally important. These spin-to-charge and charge-to-spin conversion phenomena have been described by various names in the literature, depending on the experimental details or the theoretical picture assumed. However, whether described as the spin Hall effect (SHE)^{1–4}, the Edelstein-Rashba effect^{5,6}, or a spin galvanic effect⁷, spin-orbit coupling in the spin-conversion material or at a relevant interface is essential for large effects. For this reason, heavy metals are very commonly employed for spin conversion, with sputtered platinum films remaining the workhorse material for a wide range of spin-orbit related spintronics effects and device applications^{8–11}.

Since the cost of platinum presents concerns for widespread use of these devices in information or energy technologies, finding lower cost spin conversion systems with equal or better ease of preparation is important for progress in spintronics. Spin pumping experiments, where spin excitations are driven from the nominally insulating ferromagnet yttrium iron garnet, $\text{Y}_3\text{Fe}_5\text{O}_{12}$ (YIG) into Cr films where spin-charge conversion generates a measurable voltage, were among the first to demonstrate significant spin-charge conversion in lighter metal films, including chromium¹². This study also demonstrated that spin-charge conversion in Cr generated voltage with opposite sign from both the rest of the 3d metals tested and from Pt. This work was followed shortly by studies on Cr thin films using thermal spin injection from a bulk YIG substrate^{13,14}. In this technique, often called the longitudinal spin Seebeck effect (LSSE)¹⁵, a thermal gradient applied at the interface between the nominally insulating ferromagnet YIG drives a magnon-mediated spin current toward the interface between YIG and the metallic spin conversion medium, as shown schematically in Fig. 1a. Spin-to-charge conversion generates a transverse flow of charge, which produces a detectable voltage, V_{LSSE} . One of these first works on LSSE in the Cr/YIG system investigated sputtered Cr films, with a special focus on the question of whether the antiferromagnetic ground state, observed in bulk single-crystal Cr below a Néel temperature, T_N , slightly above room temperature,¹⁶ plays a role in spin-to-charge conversion. Qu, *et al*’s measurements of V_{LSSE} vs. T showed no clear features in the range between 30 – 345 K, and the authors concluded that antiferromagnetism did not play a role in spin conversion in their Cr films. More recently, spin pumping

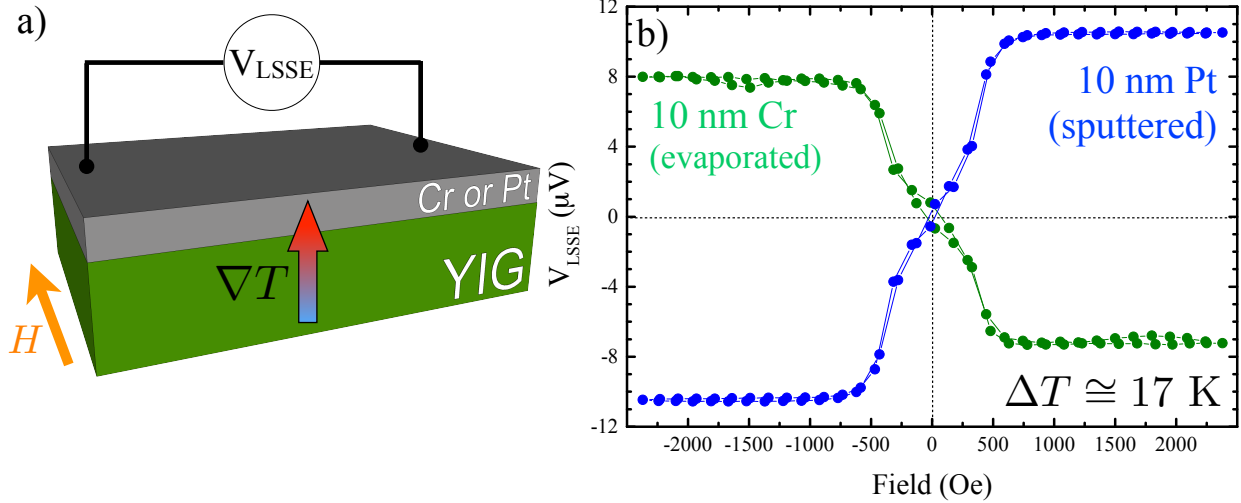


FIG. 1. a) Schematic of thermal spin injection via the longitudinal spin Seebeck effect. A thermal gradient applied to the interface between a bulk YIG substrate and Cr or Pt film drives spin current from the YIG into the metal, which is then converted to measurable transverse charge voltage, V_{LSSE} . b) V_{LSSE} vs. applied field H with a 17 K applied temperature difference for 10 nm thick evaporated Cr and sputtered Pt films. The sign of the effective spin Hall angle is reversed in Cr, which was previously observed for sputtered Cr. Evaporated Cr at the same thickness has large thermally generated signal, roughly 80% that of sputtered Pt.

experiments showed that inserting Cu between 1.2 μm thick YIG films grown via liquid-phase epitaxy and 10 nm thick sputtered Cr films dramatically reduced the signal, while keeping a negative sense of the spin-charge conversion.¹⁷ These authors argued that the spin-charge conversion in YIG/Cr is dominated by interfacial effects, commonly described as an inverse Rashba-Edelstein effect.

However, prior literature on Cr films suggests a complicated interplay of confinement, strain, and proximity effects that could play a role in spin-to-charge conversion under various circumstances. In bulk single crystals, the antiferromagnetism in Cr is the result of an incommensurate spin density wave, ISDW, where the spin of itinerant electrons is sinusoidally modulated¹⁸. The wavevector of this modulation is incommensurate with the atomic spacing of the Cr, and the direction of this wavevector orients in different direction above and below a spin-flip transition temperature near 120 K. The ISDW state affects a range of electronic properties, and is highly sensitive to impurities¹⁹. Thin films of Cr have been studied extensively²⁰, especially in the context of metallic magnetic superlattices that show oscillatory exchange coupling that is key for the giant

magnetoresistance effect^{21–23}. As direct probes of thin film antiferromagnetism are rare, the best available information on the nature of the SDW state, the resulting T_n , and its dependence on thickness and strain come from measurements of exchange bias^{24–27}. The shift in the hysteresis loop of the ferromagnetic film coupled at the interface to the AF Cr provides an important, if indirect and necessarily interface-sensitive, probe of the SDW in the Cr. Measurements of exchange bias in epitaxial Fe/Cr²⁴ and permalloy/Cr²⁵ have shown suppression of T_n with thickness. Some authors have also shown that finite size effects on the SDW state and consequently on T_n occur at surprisingly large film thickness compared to typical metallic magnetically ordered systems²⁷, with very thick films showing T_n similar to bulk single-crystal Cr, but a strongly reduced $T_n = 130$ K seen even in 25 nm thick films, a thickness large compared to expectations of typical size effects in metals. This work also showed the exchange bias was oscillatory with both temperature and thickness, since the nature of the electronic state at the interface changes due to the changing wavelength of the SDW.

Polycrystalline systems have also shown unexpected SDW phenomena, with even very early neutron scattering results indicating polycrystalline bulk samples retain a form of antiferromagnetic ordering to much higher temperatures.^{16,28} Sputtered 35 nm thick polycrystalline Cr films on permalloy similarly show no loss of ordering until 425 K, far above T_n in bulk single crystals²⁶. This occurs due to a strain state in the Cr that drives a transition from the incommensurate SDW to a *commensurate* SDW, with stronger exchange and higher ordering temperature near 475 K in absence of any finite size or grain effects. In polycrystalline thin film AF systems, the temperature probed by exchange bias is often related to the interactions between grains, called the blocking temperature, T_B . On reducing the thickness of sputtered polycrystalline films to ~ 10 nm, T_B dropped to 130 K.²⁶ These authors also identified an onset of exchange bias at Cr thickness near 6 nm. A mixed state where incommensurate and commensurate SDW coexist is also possible in polycrystalline films, and has been shown to play a role in interfacial coupling, exchange bias and other electronic properties.^{26,29} Considering the rich array of SDW phenomenology in Cr films, additional investigation of a potential role of the SDW AF state on spin conversion is needed.

Electrical resistivity, ρ , is another key property of Cr thin films relevant to spin-charge conversion. Here the literature also suggests a broad range of resistivities for various growth techniques and defects, though importantly ρ is often fairly large for a metal.³⁰ Such large ρ can be favorable for spin-charge conversion, since the spin-converting film often short circuits the transverse voltage generated from the spin conversion in various experiments. A high ρ with adequate spin-

conversion efficiency can produce useful detectors for spin currents.³¹

In this paper, we explore a new regime for Cr films for spin-charge conversion, focused on thermally evaporated polycrystalline Cr films produced in high vacuum. These films are comparatively very cheap and easy to grow, which is a distinct advantage for both fundamental studies and applications in spintronic systems. We present measurements of the LSSE and ρ for a series of films with thickness ranging from 2 – 11 nm. Both ρ and V_{LSSE} are non-monotonic with film thickness, though ρ is always much higher than seen in sputtered Cr measured by other groups. We also make a direct comparison of spin-charge conversion in our Cr films to a 10 nm thick sputtered Pt film. At the same thickness, V_{LSSE} in Cr has the opposite sign and comparable V_{LSSE} to that seen in Pt, immediately suggesting that thermally evaporated Cr can be a useful detector of spin currents.

II. EXPERIMENTAL DETAILS

We grew chromium (Cr) thin films via thermal evaporation from Cr plated tungsten rod sources in high vacuum ($\sim 10^{-6}$ Torr). We deposited Cr films with thickness, as determined by a calibrated quartz crystal mass balance, ranging from 2 to 11 nm onto 10 mm \times 2 mm \times 0.5 mm bulk polycrystalline yttrium-iron-garnet (YIG) substrates at a rate of ≈ 0.3 nm/s. An un-capped 2 nm thick Cr film, which had a measurable but high electrical resistance immediately after growth, oxidized within ~ 24 – 48 hours and was no longer measurable. Adding a thermally evaporated 2 nm thick Pd cap on the 2 nm Cr film prevented the oxidation and was used for the measurements discussed below. The samples are not intentionally heated, and remain near room temperature during growth. We attached voltage leads to the surface of the ends of these samples with indium dots, to perform resistance measurements and measurements of the LSSE voltage. We clamp each sample between two Peltier elements of length $L = 5$ mm, each containing K-type thermocouples to monitor temperature. We use these to establish a stable $\cong 17$ K temperature difference, with average sample temperature near room temperature. The resulting temperature gradient lies along the z -direction, as shown in Fig. 1. The resulting LSSE voltage is measured with a Keithley 2182 A nanovoltmeter. The clamped sample is held inside a rotatable electromagnet, aligned to apply field in the plane of the Cr film.

This type of apparatus, which is common for measuring the LSSE, robustly generates a thermal gradient at the interface between the YIG and metal film, and reliably indicates resulting spin-

charge conversion in the metal. However, comparison of resulting absolute values of the resulting V_{LSSE} have been experimentally proven not to agree well across different experimental setups and different laboratories.³² For this reason, we also prepared a comparison sample using the common spin Hall material Pt. Here we sputtered a 10 nm thick film on a polycrystalline YIG substrate of the same dimension and cut from the same larger wafer. The Pt film was sputtered after reaching base pressure of 4×10^{-8} Torr, at a rate of 0.125 nm/s at a DC sputtering power of 100 Watts. We measured the Pt/YIG sample in the same apparatus, with the same experimental conditions and measurement parameters as the Cr/YIG samples.

Electrical resistivities we report were measured with typical source-measure equipment either using 4 contacts wire-bonded near or on the indium connections after measurement of the V_{LSSE} (for T -dependent data reported in Fig. 3 below), or using the same 2-wire leads as the V_{LSSE} measurements (shown in Fig. 4 below)

III. RESULTS AND DISCUSSION

Figure 1b compares V_{LSSE} vs applied field H for 10 nm thick evaporated Cr (green symbols) and sputtered Pt films (blue symbols). This shows reversal of the sign of the spin-charge conversion generated voltage, as expected, but also a large total voltage in evaporated Cr, which retains 80% of the signal of sputtered Pt. The ratio of these voltages suggests potentially larger spin conversion in this evaporated film compared to sputtered Cr, where the spin Hall angle, θ_{sh} , measured via similar thermal spin injection from polycrystalline YIG was previously reported to be only $\approx 30\%$ of Pt.¹⁴ Note that the somewhat large coercivity and complicated reversal patterns are typical for the bulk polycrystalline YIG substrates we use as a spin source.^{33,34}

Figure 2 compares V_{LSSE} vs. H for a series of Cr films of different thickness ranging from 2 to 11 nm. The simplest expectations of bulk spin to charge conversion suggest a monotonic drop in V_{LSSE} with growing film thickness. However, the evaporated Cr does not show this trend, seen clearly since the Cr/YIG samples in the middle range of thickness are plotted on larger voltage scales (indicated with a dashed line). For the 10 nm thick values, we also compare V_{LSSE} in an as-grown sample and in a second sample measured after vacuum annealing at $\sim 100^\circ$ C for 2 hours. Annealing caused only slight shifts in V_{LSSE} and ρ (shown below). The excellent agreement between these two separate 10 nm thick samples also indicates that both the growth of the Cr and the measurement techniques are robust and repeatable.

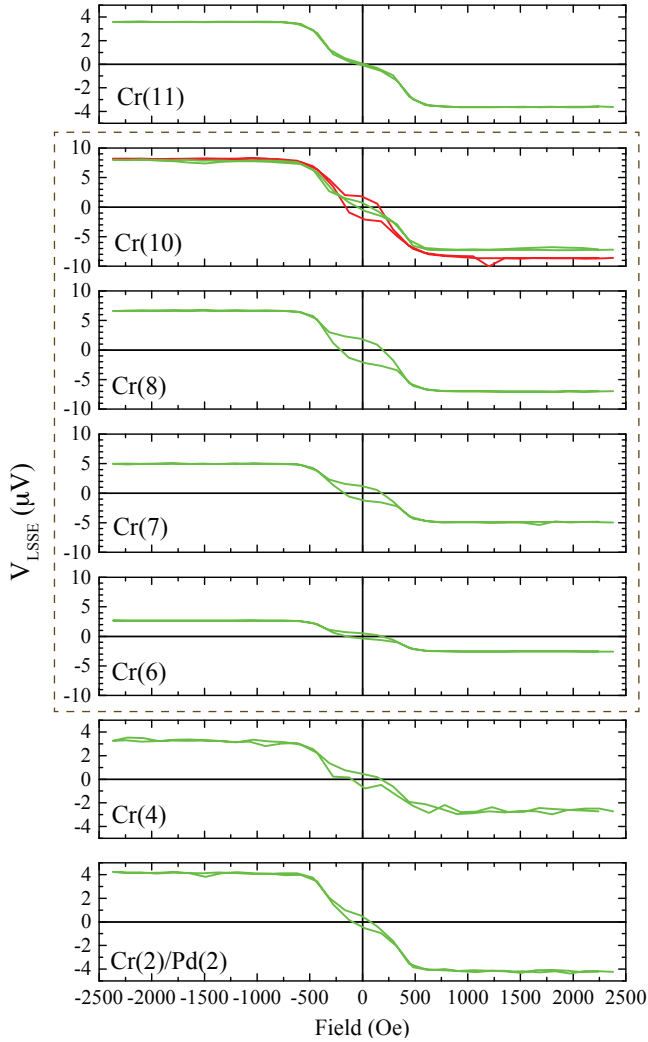


FIG. 2. V_{LSSE} vs. H for eight Cr/YIG films with thickness (indicated in nanometers by the number in parenthesis) ranging from 2 – 11 nm. The thinnest Cr film is capped with Pd to prevent oxidation. Two 10 nm thick samples are shown, one (red line) that was annealed at $\sim 100^\circ \text{ C}$ in vacuum for 2 hours after growth. Note the plots in the dashed box are plotted on larger voltage scale than the other three plots.

Figure 3 plots electrical resistivity, ρ , vs. T measured in a 4-wire configuration for the 6 nm and 10 nm thick Cr samples. The evaporated Cr films show large values of resistivity, which is not unusual for Cr films, which are known to demonstrate a high degree of sensitivity to defects and film morphology.^{20,29,30} The 10 nm thick film has essentially constant ρ vs. T , and the thinner 6 nm thick film shows ρ larger at low T . This negative slope of ρ with T is not typical for a metal, but often observed in Cr for certain ranges of T when various impurity atoms are added.¹⁹ Despite ρ much larger than the measured value for the 10 nm thick sputtered Pt film on YIG

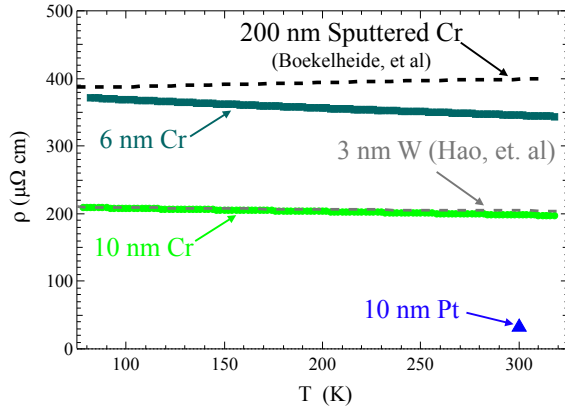


FIG. 3. Charge resistivity vs. T for two Cr films and Pt, measured on the same samples as V_{LSSE} , compared to literature values for 200 nm thick sputtered Cr³⁰, and a previously established negative spin-charge conversion material, 3 nm thick tungsten.³¹ Both evaporated Cr films have large values.

(blue triangle), the Cr films still have smaller ρ compared to some polycrystalline films, such as the much thicker 200 nm sputtered film (black dashed line)³⁰. Both evaporated Cr films have ρ consistent with large values of residual resistivity, which in some studies has been correlated with mixed SDW state.^{29,30} These values of ρ are also comparable to those seen in other negative spin Hall angle materials such as tungsten (grey dashed line).³¹ In both cases the large charge resistivity contributes to large spin-charge conversion.

In Fig. 4a) we plot the saturated absolute value of spin Seebeck voltage, $|V_{\text{LSSE}}| = |V_{\text{LSSE}}(+H_{\text{sat}}) - V_{\text{LSSE}}(-H_{\text{sat}})|$ vs. the thickness of the metallic layer for our evaporated Cr/YIG, our sputtered 10 nm Pt/YIG reference sample, and literature data for sputtered Cr.¹⁴ Here we rescaled the literature data to match the $\sim 1.7 \times$ higher applied thermal gradient used in our experiment; the published values for sputtered Cr are somewhat lower. The evaporated Cr spin-charge conversion is non-monotonic with thickness in this range, and does not follow the simple expectations of a modified $1/t$ dependence. Instead, the values become sharply larger above 6 nm, the same thickness where polycrystalline Cr on Py showed an onset of exchange bias.²⁶ This jump results in large spin conversion voltages, which not only grow larger than seen in sputtered Cr, but also (as also shown in Fig. 1) become comparable to Pt. With additional thickness, V_{LSSE} for evaporated Cr then drops sharply back to values in line with the thinner films.

Fig. 4b) compares ρ v. t measured near room temperature for the same set of samples. The

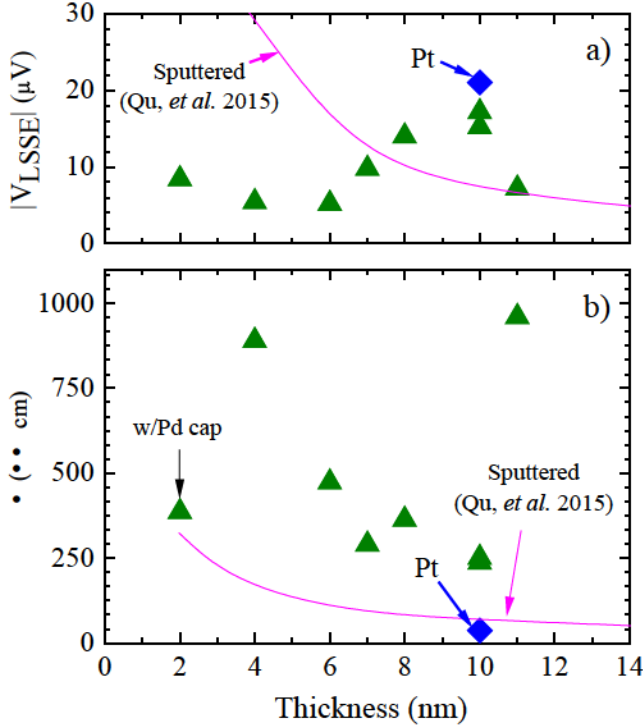


FIG. 4. **a)** Absolute value of saturated V_{LSSE} vs. thickness comparing evaporated Cr (green triangles) and 10 nm thick Pt to literature values for sputtered Cr (scaled to equal applied ∇T).¹⁴ Estimated uncertainty is $\sim 5 - 10\%$, on order of the size of the data points. **b)** Charge resistivity, ρ vs. thickness measured on the same samples, again comparing to literature Cr values.

uncapped evaporated Cr samples all show much larger ρ , which is again non-monotonic with t , though with a different pattern than seen in V_{LSSE} . As noted in the annotation, the thinnest Cr film was capped with Pd, and this is most likely the main cause of the lower value for that sample. Though Pd has large spin-orbit coupling and has been reported to show significant spin-charge conversion in some samples,^{35,36} an evaporated Pd/YIG sample showed $> 10\times$ lower V_{LSSE} than any of the evaporated Cr samples. As a result we expect the main effect of the cap is to reduce ρ while not contributing significant spin conversion that would modify V_{LSSE} .

Fig. 5 compares the same samples using a measure of the overall spin-charge conversion, based on the typical theoretical analysis of the spin Seebeck effect. Thermally generated spin voltage, with the assumption of spin-charge conversion occurring in the bulk of the film via the spin Hall effect, is typically described by:

$$V_{\text{LSSE}} = 2(C\text{L}\nabla T)(\rho\theta_{\text{sh}})\frac{\lambda_{\text{sf}}}{t} \tanh\left(\frac{t}{2\lambda_{\text{sf}}}\right), \quad (1)$$

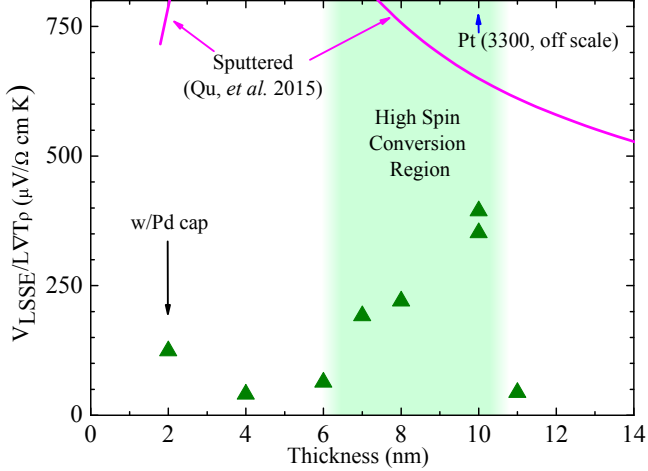


FIG. 5. Comparison of the spin conversion efficiency, $V_{\text{LSSSE}}/LVT\rho$ for literature values of sputtered Cr and evaporated Cr. In the highlighted regime between 6 and 11 nm, the evaporated Cr develops a much larger spin-conversion efficiency, reaching $\sim 1/2$ the values reported for sputtered Cr at the same thickness. Pt at 10 nm has the largest efficiency value, at $3300 \mu\text{V}/\Omega\text{cmK}$.

where ∇T is the applied thermal gradient, ρ is the charge resistivity, θ_{sh} is the spin Hall angle, λ_{sf} is the spin diffusion length in the metal film, t is the film thickness, and C is a constant related to the efficiency of spin injection from the YIG to the metal film.^{14,33,34} Here three trivial methods of increasing the thermal signal are obvious: increasing ∇T , increasing L (which increases V_{LSSSE} simply by integrating the same electric field over a longer path), and increasing ρ (which reduces simple electrical shorting of the generated voltage by charge flow in the metal film). Rewriting Eq. 1 gives:

$$\frac{V_{\text{LSSSE}}}{LVT\rho} = 2(C\theta_{\text{sh}}) \frac{\lambda_{\text{sf}}}{t} \tanh\left(\frac{t}{2\lambda_{\text{sf}}}\right), \quad (2)$$

such that the right-hand side depends only on t and spin-related properties of the heterostructure. Comparison of the quantity $|V_{\text{LSSSE}}|/LVT\rho$ between samples therefore removes the three trivial effects. With this view of spin-charge conversion, we see that both sputtered and evaporated Cr have much lower spin-conversion efficiency than Pt (which falls at $3300 \mu\text{V}/\Omega\text{ cm K}$, much higher than the range plotted in Fig. 5), but that the evaporated Cr retains roughly half the spin-charge conversion efficiency of sputtered Cr between 6 – 11 nm.

As shown by the literature data for sputtered Cr, when well-described by Eq. 2, λ_{sf} and θ_{sh} can be determined from this data. As shown in Fig. 5, the evaporated Cr/YIG samples do not obey Eq. 2, instead showing essentially the same non-monotonic pattern seen in V_{LSSSE} , again with

sudden increase in spin conversion above 6 nm and sudden drop below 11 nm. This behavior with thickness suggests, as seen in earlier reports on exchange bias, that the evolution of strain in the evaporated film modifies the nature of the spin density wave, which in turn causes the sudden changes in spin-charge conversion. From our experiments we cannot determine if this change is driven by modified coupling at the interface (represented here as a changing C parameter), a change in the spin conversion itself (a changing θ_{sf}), or a change in λ_{sf} . Indeed, the modification in the Fermi surface that is expected based on strain-induced changes of the nature of the spin density wave in Cr could affect any or all of these parameters. As the strain state of evaporated and sputtered films are generally very different,³⁷⁻³⁹ strain is a likely explanation of the very different charge and spin properties of evaporated and sputtered Cr films.

IV. CONCLUSIONS

In summary, we presented evidence of large negative spin-charge conversion in evaporated Cr films on polycrystalline YIG substrates using the spin Seebeck effect. The large thermally-driven spin voltages, which are larger than those previously seen in sputtered Cr for some thicknesses, are partly achieved due to large charge resistivity, which is comparable to negative spin-charge conversion materials demonstrated by others. A non-monotonic pattern in both the unscaled V_{LSSE} and that scaled by ρ for evaporated Cr suggests, as previously seen in exchange bias experiments in Cr heterostructures, that changing thickness changes the film strain, which modifies the nature of the spin density wave electronic state of Cr, modifying the spin-charge conversion process. This demonstrates that, for thicknesses chosen in the optimal range, cheap and easy to prepare evaporated Cr films can be useful spin detectors in a range of spintronic and spincaloritronic measurements and applications.

ACKNOWLEDGMENTS

We thank C. Leighton, Y. Takamura, and D. Balzar for helpful discussions, and gratefully acknowledge support from the NSF (No. DMR-2004646). The bulk of this work was performed on lands traditionally held by the Cheyenne and Arapaho nations.

V. DATA AVAILABILITY

The data that support the findings of this study are available from the corresponding author upon reasonable request.

REFERENCES

- ¹M. Dyakonov and V. Perel, “Current-induced spin orientation of electrons in semiconductors,” *Physics Letters A* **35**, 459 – 460 (1971).
- ²J. E. Hirsch, “Spin Hall effect,” *Phys. Rev. Lett.* **83**, 1834–1837 (1999).
- ³A. Hoffmann, “Spin Hall effects in metals,” *Magnetics, IEEE Transactions on* **49**, 5172–5193 (2013).
- ⁴J. Sinova, S. O. Valenzuela, J. Wunderlich, C. H. Back, and T. Jungwirth, “Spin Hall effects,” *Rev. Mod. Phys.* **87**, 1213–1260 (2015).
- ⁵V. Edelstein, “Spin polarization of conduction electrons induced by electric current in two-dimensional asymmetric electron systems,” *Solid State Communications* **73**, 233–235 (1990).
- ⁶J. C. R. Sánchez, L. Vila, G. Desfonds, S. Gambarelli, J. P. Attané, J. M. D. Teresa, C. Magén, and A. Fert, “Spin-to-charge conversion using Rashba coupling at the interface between non-magnetic materials,” *Nature Communications* **4**, 2944 (2013).
- ⁷S. D. Ganichev, E. L. Ivchenko, V. V. Bel’kov, S. A. Tarasenko, M. Sollinger, D. Weiss, W. Wegscheider, and W. Prettl, “Spin-galvanic effect,” *Nature* **417**, 153–156 (2002).
- ⁸G. Y. Guo, S. Murakami, T.-W. Chen, and N. Nagaosa, “Intrinsic spin Hall effect in platinum: First-principles calculations,” *Phys. Rev. Lett.* **100**, 096401 (2008).
- ⁹L. Liu, R. A. Buhrman, and D. Ralph, “Review and analysis of measurements of the spin Hall effect in platinum,” *cond-mat arXiv:1111.3702v3* (2011).
- ¹⁰M.-H. Nguyen, D. C. Ralph, and R. A. Buhrman, “Spin torque study of the spin Hall conductivity and spin diffusion length in platinum thin films with varying resistivity,” *Phys. Rev. Lett.* **116**, 126601 (2016).
- ¹¹E. Sagasta, Y. Omori, M. Isasa, M. Gradhand, L. E. Hueso, Y. Niimi, Y. Otani, and F. Casanova, “Tuning the spin hall effect of Pt from the moderately dirty to the superclean regime,” *Phys. Rev. B* **94**, 060412 (2016).

¹²C. Du, H. Wang, F. Yang, and P. C. Hammel, “Systematic variation of spin-orbit coupling with *d*-orbital filling: Large inverse spin Hall effect in 3*d* transition metals,” *Phys. Rev. B* **90**, 140407 (2014).

¹³K. Uchida, M. Ishida, T. Kikkawa, A. Kirihara, T. Murakami, and E. Saitoh, “Longitudinal spin Seebeck effect: from fundamentals to applications,” *Journal of Physics: Condensed Matter* **26**, 343202 (2014).

¹⁴D. Qu, S. Y. Huang, and C. L. Chien, “Inverse spin Hall effect in Cr: Independence of antiferromagnetic ordering,” *Phys. Rev. B* **92**, 020418 (2015).

¹⁵K. i. Uchida, H. Adachi, T. Kikkawa, A. Kirihara, M. Ishida, S. Yorozu, S. Maekawa, and E. Saitoh, “Thermoelectric generation based on spin Seebeck effects,” *Proceedings of the IEEE* **104**, 1946–1973 (2016).

¹⁶G. E. Bacon, “A neutron-diffraction study of very pure chromium,” *Acta Crystallographica* **14**, 823–829 (1961).

¹⁷L. Ni, Z. Chen, X. Lu, Y. Yan, L. Jin, J. Zhou, W. Yue, Z. Zhang, L. Zhang, W. Wang, Y.-L. Wang, X. Ruan, W. Liu, L. He, R. Zhang, H. Zhang, B. Liu, R. Liu, H. Meng, and Y. Xu, “Strong interface-induced spin-charge conversion in YIG/Cr heterostructures,” *Applied Physics Letters* **117**, 112402 (2020).

¹⁸E. Fawcett, “Spin-density-wave antiferromagnetism in chromium,” *Rev. Mod. Phys.* **60**, 209–283 (1988).

¹⁹E. Fawcett, H. L. Alberts, V. Y. Galkin, D. R. Noakes, and J. V. Yakhmi, “Spin-density-wave antiferromagnetism in chromium alloys,” *Rev. Mod. Phys.* **66**, 25–127 (1994).

²⁰H. Zabel, “Magnetism of chromium at surfaces, at interfaces and in thin films,” *Journal of Physics: Condensed Matter* **11**, 9303–9346 (1999).

²¹S. S. P. Parkin, N. More, and K. P. Roche, “Oscillations in exchange coupling and magnetoresistance in metallic superlattice structures: Co/Ru, Co/Cr, and Fe/Cr,” *Phys. Rev. Lett.* **64**, 2304–2307 (1990).

²²J. Unguris, R. J. Celotta, and D. T. Pierce, “Observation of two different oscillation periods in the exchange coupling of Fe/Cr/Fe(100),” *Phys. Rev. Lett.* **67**, 140–143 (1991).

²³C. D. Potter, R. Schad, P. Beliën, G. Verbanck, V. V. Moshchalkov, Y. Bruynseraede, M. Schäfer, R. Schäfer, and P. Grünberg, “Two-monolayer-periodicity oscillations in the magnetoresistance of Fe/Cr/Fe trilayers,” *Phys. Rev. B* **49**, 16055–16057 (1994).

²⁴E. E. Fullerton, K. T. Riggs, C. H. Sowers, S. D. Bader, and A. Berger, “Suppression of bi-quadratic coupling in Fe/Cr(001) superlattices below the Néel transition of Cr,” *Phys. Rev. Lett.* **75**, 330–333 (1995).

²⁵F. Y. Yang and C. L. Chien, “Oscillatory exchange bias due to an antiferromagnet with incommensurate spin-density waves,” *Physical Review Letters* **90** (2003), 10.1103/physrevlett.90.147201.

²⁶F. Y. Yang and C. L. Chien, “Exchange coupling between Cr and ferromagnetic thin films,” *Journal of Applied Physics* **93**, 6829–6831 (2003).

²⁷J. S. Parker, L. Wang, K. A. Steiner, P. A. Crowell, and C. Leighton, “Exchange bias as a probe of the incommensurate spin-density wave in epitaxial Fe/Cr(001),” *Phys. Rev. Lett.* **97**, 227206 (2006).

²⁸C. G. Shull and M. K. Wilkinson, “Neutron diffraction studies of various transition elements,” *Rev. Mod. Phys.* **25**, 100–107 (1953).

²⁹Z. Boekelheide, E. Helgren, and F. Hellman, “Spin-density wave in polycrystalline Cr films from infrared reflectivity,” *Phys. Rev. B* **76**, 224429 (2007).

³⁰Z. Boekelheide, D. W. Cooke, E. Helgren, and F. Hellman, “Resonant impurity scattering and electron-phonon scattering in the electrical resistivity of Cr thin films,” *Physical Review B* **80** (2009).

³¹Q. Hao, W. Chen, and G. Xiao, “Beta (β) tungsten thin films: Structure, electron transport, and giant spin Hall effect,” *Applied Physics Letters* **106**, 182403 (2015).

³²A. Sola, V. Basso, M. Kuepferling, M. Pasquale, D. C. ne Meier, G. Reiss, T. Kuschel, T. Kikkawa, K. ichi Uchida, E. Saitoh, H. Jin, S. J. Watzman, S. Boona, J. Heremans, M. B. Jungfleisch, W. Zhang, J. E. Pearson, A. Hoffmann, and H. W. Schumacher, “Spincaloritronic measurements: A round robin comparison of the longitudinal spin Seebeck effect,” *IEEE Transactions on Instrumentation and Measurement* **68**, 1765–1773 (2019).

³³D. Qu, S. Y. Huang, J. Hu, R. Wu, and C. L. Chien, “Intrinsic spin Seebeck effect in Au/YIG,” *Phys. Rev. Lett.* **110**, 067206 (2013).

³⁴D. Qu, S. Y. Huang, B. F. Miao, S. X. Huang, and C. L. Chien, “Self-consistent determination of spin Hall angles in selected 5d metals by thermal spin injection,” *Phys. Rev. B* **89**, 140407 (2014).

³⁵K. Ando and E. Saitoh, “Inverse spin-Hall effect in palladium at room temperature,” *Journal of Applied Physics* **108**, 113925 (2010).

³⁶Z. Tang, Y. Kitamura, E. Shikoh, Y. Ando, T. Shinjo, and M. Shiraishi, “Temperature dependence of spin Hall angle of palladium,” *Applied Physics Express* **6**, 083001 (2013).

³⁷J. A. Thornton and D. Hoffman, “Stress-related effects in thin films,” *Thin Solid Films* **171**, 5–31 (1989).

³⁸R. Koch, “Stress in evaporated and sputtered thin films: A comparison,” *Surface and Coatings Technology* **204**, 1973–1982 (2010).

³⁹G. Abadias, E. Chason, J. Keckes, M. Sebastiani, G. B. Thompson, E. Barthel, G. L. Doll, C. E. Murray, C. H. Stoessel, and L. Martinu, “Review article: Stress in thin films and coatings: Current status, challenges, and prospects,” *Journal of Vacuum Science & Technology A* **36**, 020801 (2018).